DOI: 10.1534/genetics.109.101055

Both the RGS Domain and the Six C-Terminal Amino Acids of Mouse Axin Are Required for Normal Embryogenesis

Ian V. Chia,* Min Jung Kim,* Keiji Itoh,† Sergei Y. Sokol† and Frank Costantini*,[1]

**Department of Genetics and Development, Columbia University Medical Center, New York, New York 10032 and*
†*Department of Developmental and Regenerative Biology, Mount Sinai School of Medicine, New York, New York 10029*

Manuscript received January 22, 2009
Accepted for publication February 3, 2009

ABSTRACT

Axin is a negative regulator of canonical Wnt signaling, which promotes the degradation of β-catenin, the major effector in this signaling cascade. While many protein-binding domains of Axin have been identified, their significance has not been evaluated *in vivo*. Here, we report the generation and analysis of mice carrying modified *Axin* alleles in which either the RGS domain or the six C-terminal amino acids (C6 motif) were deleted. The RGS domain is required for APC-binding, while the C6 motif has been implicated in the activation of c-Jun N-terminal kinase, but is not required for the effects of Axin on the Wnt/β-catenin pathway, *in vitro*. Both mutant *Axin* alleles caused recessive embryonic lethality at E9.5–E10.5, with defects indistinguishable from those caused by a null allele. As Axin-ΔRGS protein was produced at normal levels, its inability to support embryogenesis confirms the importance of interactions between Axin and APC. In contrast, Axin-ΔC6 protein was expressed at only 25–30% of the normal level, which may account for the recessive lethality of this allele. Furthermore, many $Axin^{\Delta C6/\Delta C6}$ embryos that were heterozygous for a β-catenin null mutation survived to term, demonstrating that early lethality was due to failure to negatively regulate β-catenin.

AXIN is a key negative regulator of the canonical Wnt signaling pathway (Zeng *et al.* 1997), which functions by promoting the degradation of β-catenin, the major effector in the signaling cascade (Luo and Lin 2004). The related protein Axin2/Conductin is thought to function similarly (Behrens *et al.* 1998), and appears to have partially overlapping roles in development. Loss of *Axin* results in early embryonic lethality (Zeng *et al.* 1997), while *Axin2* null mice are viable but display skull malformations (Yu *et al.* 2005). Mutations in both genes are associated with cancer in humans (Salahshor and Woodgett 2005). The lack of redundancy between *Axin* and *Axin2* is apparently due to their different modes of expression: while *Axin* is expressed ubiquitously (Zeng *et al.* 1997), *Axin2* is expressed in a tissue- and developmental stage-specific pattern, and its transcription is induced by canonical Wnt signaling (Jho *et al.* 2002; Lustig *et al.* 2002; Aulehla *et al.* 2003). The functional equivalence of Axin and Axin2 *in vivo* was established by generating knockin mice in which the *Axin* gene was replaced with an Axin2 cDNA. The mutant mice, which expressed no endogenous Axin, but produced Axin2 under control of the *Axin* locus, were phenotypically normal (Chia and Costantini 2005).

[1]*Corresponding author:* Department of Genetics and Development, Columbia University Medical Center, 701 W. 168th St., New York, NY 10032. E-mail: fdc3@columbia.edu

Axin has a number of domains that interact with other proteins, many of which are known to be involved in canonical Wnt signaling (*e.g.*, GSK3, β-catenin, Dvl, and LRP5/6), but some of which are not (*e.g.*, MEKK1, MEKK4, Smad3, and I-mfa) (Fagotto *et al.* 1999; Hsu *et al.* 1999; Jho *et al.* 1999; Kishida *et al.* 1999; Li *et al.* 1999; Yamamoto *et al.* 1999; Julius *et al.* 2000; Mao *et al.* 2001; Luo and Lin 2004). While the locations of many protein-binding domains of Axin have been determined, the functional significance of many of these domains is unclear. Most previous structure–function studies of Axin used a gain-of-function approach, in which an altered form of Axin was overexpressed in cell lines or frog embryos, in the presence of endogenous wild-type Axin and assayed for its ability to regulate β-catenin signaling or embryonic axis formation. To test the importance of different domains of Axin under physiological conditions, we have used a knockin approach to generate mutant alleles of the mouse *Axin* locus, and ask if they could support normal development *in vivo*. Our strategy was based on the demonstration that replacement of the *Axin* gene by a Myc-tagged Axin (or Axin2) cDNA, by targeting in embryonic stem (ES) cells, was not only efficient, but produced mice with no apparent abnormalities.

The two domains we examine here are the "RGS domain" in the N-terminal region and the KVEKVD motif at the C terminus (Figure 1A). The RGS domain of Axin, although named for its sequence similarity to

*r*egulators of *G*-protein *s*ignaling, is thought to be important primarily as the binding site for APC (Hart *et al.* 1998; Ikeda *et al.* 1998; Julius *et al.* 2000). APC is another important regulator of β-catenin levels, and mutations in APC are found in colon tumor cells with high levels of β-catenin and constitutively active TCF/β-catenin nuclear complexes (Munemitsu *et al.* 1995). The addition of exogenous wild-type APC into APC-null colon carcinoma cells reduces β-catenin levels, and antagonizes TCF/β-catenin-mediated transcription, demonstrating that APC negatively regulates β-catenin levels (Korinek *et al.* 1997). Surprisingly, it was reported that Axin is capable of degrading β-catenin when overexpressed in cells that lack functional APC (Hart *et al.* 1998). This indicates that Axin can also function downstream from, or independently of, APC, at least when overexpressed. From crystal structure studies, it was proposed that upon phosphorylation by GSK3 in the degradation complex, the affinity of APC for β-catenin increases and allows APC to compete with Axin for binding to β-catenin. In doing so, APC causes the release of β-catenin from Axin. Next, PP2A dephosphorylates APC such that phosphorylated β-catenin is freed from APC, and the destruction complex is made available for another β-catenin molecule to be targeted for degradation (Xing *et al.* 2003).

Xenopus embryo injection assays using a form of Axin lacking the RGS domain (Axin-ΔRGS) showed that it behaves in a dominant-negative fashion and stabilizes β-catenin instead of degrading it (Zeng *et al.* 1997; Itoh *et al.* 1998). In another study, however, the RGS domain appeared to be dispensable, as a truncated form of Axin lacking this domain was capable of downregulating β-catenin in a cell culture assay (Hart *et al.* 1998). To resolve this issue with an *in vivo* assay, we generated mice with an Axin-ΔRGS knockin allele ($Axin^{\Delta RGS}$).

The second domain we study consists of six amino acids (KVEKVD) at the extreme C terminus of Axin (hereafter called the C6 motif). This sequence is identical in mouse, rat, and human Axin, and differs by only one amino acid in chick (KVEKID) or frog (QVEKID). It was reported that overexpression of Axin in HEK 293T cells activates the c-Jun N-terminal kinase (JNK) through domains distinct from those involved in Wnt signaling (Zhang *et al.* 1999) and that the C6 motif was one of the domains required for JNK activation (Rui *et al.* 2002). The deletion of the C6 motif impaired the ability of Axin to activate JNK, without affecting its ability to homodimerize or to function in the Wnt/β-catenin pathway. In addition to its potential role in JNK activation, the C6 motif is critical for the interaction of Axin with SUMO1-conjugating E3 enzymes, and it includes two lysine residues that were the main sites for the SUMOylation of Axin when Axin was cotransfected with HA-tagged SUMO (Rui *et al.* 2002). Because the importance of Axin for JNK activation during normal development was unclear, as was the role of C-terminal SUMOylation in the functions of Axin, we generated a mutant *Axin* allele (designated $Axin^{\Delta C6}$) lacking these six residues.

MATERIALS AND METHODS

Targeting vectors, ES cells, mice and embryonic fibroblasts: Two targeting vectors flanked by *Axin* homology arms, $pMTAX^{\Delta RGS}$ and $pMTAX^{\Delta C6}$, were constructed for the generation of mutant alleles (Figure 1B), as described (Chia and Costantini 2005). For the construction of $pMTAX^{\Delta RGS}$, myc-tagged AxinΔRGS cDNA was excised from pCS2-MT + AxinΔRGS using *Cla*I and *Not*I, the ends blunted, and cloned into the *Cla*I site of pBluescript IISK, as described for construction of the pMTAX targeting vector (Chia and Costantini 2005). To create Myc-tagged AxinΔC6 cDNA, two sets of PCR reactions were performed simultaneously using primers AXSPE (GCTATTCCGAGAACGCAGGCAC) and mutSUMO (CTGCCCAGTGCTCAGCCGATGATCTTTT CTTCAAAGACAGG) and SUMOend3 (TGAGCACTGGG CAGCACAC) and T3 (AATTAACCCTCACTAAAGGG) on pCS2-MT + Axin as a template. The products of the two PCR reactions were then annealed and used as templates for another round of PCR using primers AXSPE and T3. The final PCR product was cut with *Spe*I and *Sac*II and subcloned into pCS2-MT + Axin that had also been digested with *Spe*I and *Sac*II. This new vector is pCS2-MT + AxinΔC6. To create the targeting vector $pMTAX^{\Delta C6}$, Myc-tagged Axin-ΔC6 cDNA was excised from pCS2-MT + AxinΔC6 using *Cla*I and *Not*I, ends blunted, and cloned into the *Cla*I site of pBluescriptIISK, as described for construction of the pMTAX vector (Chia and Costantini 2005).

The targeting vectors were linearized with *Not*I and electroporated into CSL3 ES cells (derived from strain 129/SvEv, a gift of Victor Lin), which were selected with 0.35 mg/ml G418. DNA from surviving colonies was digested with *Hpa*I and screened by Southern blot using a 479-bp probe, PB (see Figure 1B), generated by PCR of genomic DNA with primers 5′-CTTCTAATGGTATGAGGCTG-3′ and 5′-GCATCTGCACT TGCCATCTAC-3′ (Chia and Costantini 2005). This probe is located outside the homology arms of the targeting vector, so the change in band size in mutant clones must reflect a recombination event that altered the structure of the endogenous *Axin* locus. By the criteria of Southern blotting, correctly targeted clones were isolated for both alleles (Figure 1C), with targeting frequencies of 9/300 and 8/300 for $pMTAX^{\Delta RGS}$ and $pMTAX^{\Delta C6}$, respectively.

Two $Axin^{\Delta RGS}$ ES clones (R1 and R24) and two $Axin^{\Delta C6}$ ES clones (S58 and S191) were injected into C57BL/6J (B6) blastocysts. Highly chimeric males made with clones R1, R24, and S58 were mated to B6 females to obtain initial germline transmission, and to β-actin-Cre transgenic females (Lewandoski 2001) to obtain progeny in which the PGK-neo cassette was removed (Figure 1B). Mice and embryos were genotyped by PCR (Figure 1D) using the following primers: AXL1 (5′-GGACCACCTTTCCTAATCCTTG-3′) and MTAXR1 (5′-AACCCTGCTCCTGGACATTC-3′), which amplify the wild type (146 bp) and the $AX^{\Delta X}$, $AX^{\Delta RGS}$, and $AX^{\Delta C6}$ (404 bp) alleles, at annealing temperature 56.5°. To generate a null allele of *Ctnnb1*, we crossed a floxed allele (Brault *et al.* 2001) to a germ-line Cre strain (Lewandoski and Martin 1997).

Mouse embryonic fibroblasts (MEFs) were prepared from E13.5 embryos of various genotypes and cultured in Dulbecco's modified Eagle's medium (DMEM, Sigma) supplemented with 10% heat-inactivated fetal bovine serum (FBS, HyClone Laboratories) and 50 μg/ml penicillin and streptomycin (GIBCO) in 5% CO_2 at 37°.

RT-PCR: Total RNA was prepared from MEFs using TRIzol (Ambion) and used for RT–PCR with a pair of primers specific for Axin, AXL2 (5′-GAGATTGATTCCCTTGGGAGC-3′) and MTAXR1 (5′-AACCCTGCTCCTGGACATTC-3′) (Chia and Costantini 2005). The reactions were run at 94° (1 min), 65° (40 sec), and 72° (1 min) for 30 cycles.

Western blots: Embryos were dissected at E10.5 and homogenized as described (Fagotto *et al.* 1999). Protein lysates were prepared from MEFs using RIPA buffer as described (Kim *et al.* 2008). The anti-Axin polyclonal antibody (against full-length mouse Axin) was from David Virshup and used at a dilution of 1/20,000.

JNK assays: MEFs from wild type, *Axin*$^{\Delta C6/\Delta C6}$;*Ctnnb1*+/−, or *Ctnnb1*+/− E13.5 embryos were cultured in DMEM, UV irradiated (100 mJ/m^2) and lysed with nondenaturing cell lysis buffer (Cell Signaling no. 9803) plus 1 mm PMSF after incubation for 0, 0.5, 1, or 2 hr. JNK assays were conducted with PathScan Phospho SAPK/JNK (Thr183/Tyr185) Sandwich ELISA kit and Total SAPK/JNK Sandwich ELISA kit (Cell Signaling).

Xenopus embryo experiments: Micro-injections of RNAs into *Xenopus laevis* embryos were carried out as described (Itoh *et al.* 1998). RNAs for micro-injection were transcribed *in vitro* from pCS2-MT + Axin and pCS2-MT + AxinΔ6 linearized with *Sac*II using mMessage mMachine SP6 kit (Ambion). To monitor ventralizing activities of Axin constructs, RNAs at the dose of 0.7 or 2 ng were injected into two dorsovegetal blastomeres of 4–8 cell embryos. Injected embryos were scored according to dorsoanterior index (DAI) (Kao and Elinson 1988) when uninjected control embryos reached stage 36. DAI 5 is scored as normal; DAI 4, reduced eyes and forehead; DAI 3, cyclopic; DAI 2, microcephalic; DAI 1, acephalic, and DAI 0, no dorsal axial structures. Two experiments were performed with essentially the same results. To assess protein expression levels, Western blot analysis of embryo lysates was carried out with anti-Myc antibodies as described (Itoh *et al.* 1998), when uninjected sibling embryos reached early gastrula stage.

DNA Sequencing: Two primers flanking the C-terminal region of Axin cDNA (pDIX: CACCATGTGACAGCATTG and DIXp: TGTCCACCTGACTGATGAC) were used for PCR amplification of genomic DNA from *Axin*$^{Ax/+}$ and *Axin*$^{\Delta C6/+}$ mouse tails. The products were subcloned and sequenced. Primers pDIX and DIXp are located in different exons and therefore the PCR product is only amplified from knockin cDNA and not endogenous *Axin*.

RESULTS

Generation of *Axin*$^{\Delta RGS}$ and *Axin*$^{\Delta C6}$ mutant alleles: The targeting strategy (Figure 1B and materials and methods) was similar to that previously used to replace the *Axin* gene with wild-type Axin or Axin2 cDNAs, including a Myc-tag at the N terminus (Chia and Costantini 2005). Correctly targeted ES cell clones were identified by Southern blotting (Figure 1C and data not shown), and transmission of the wild-type and mutant alleles was detected by PCR (Figure 1D). Although the *neo* cassette had no apparent effect on Axin expression levels or on the mutant phenotypes, it was removed by crossing mice carrying the targeted *Axin* alleles to a β-*actin*/Cre recombinase transgenic line (Lewandoski and Martin 1997).

To determine the level of expression of the *Axin*$^{\Delta C6}$ and *Axin*$^{\Delta RGS}$ alleles, protein extracts from heterozygous embryos (in which the endogenous Axin serves as an internal control) were analyzed by Western blotting with anti-Axin antibodies. Mouse embryos heterozygous for the *Axin*^{Ax} allele (which contains a wild-type, Myc-tagged Axin cDNA inserted at the *Axin* locus) expressed levels of Myc-tagged Axin (which is ~20 kDa larger due to the addition of six Myc epitopes) approximately equal to, or slightly higher than, endogenous Axin (Figure 1E, lane 3). Therefore, the presence of the Myc tag, or the use of a cDNA sequence to encode Axin, does not reduce the level of expression compared to that encoded by the normal allele, as reported previously (Chia and Costantini 2005). However, we found that the level of the Axin-ΔC6 protein was three- to fourfold lower than the endogenous Axin in heterozygous *Axin*$^{\Delta C6/+}$ embryos (Figure 1E, lanes 4 and 5) or *Axin*$^{\Delta C6/+}$ MEFs (Figure 1F, lane 2). In contrast, the level of Axin-ΔC6 mRNA was equivalent to that of endogenous Axin mRNA, as shown by RT–PCR (Figure 1G), suggesting that the Axin-ΔC6 protein was either inefficiently translated or less stable than wild-type Myc-tagged Axin. While the presence of a six-amino-acid deletion at the C terminus is unlikely to affect translational efficiency, Axin-ΔC6 protein was found to have a reduced half-life (Kim *et al.* 2008), which largely accounts for its reduced steady-state level. Surprisingly, Axin-ΔC6 protein was below the limit of detection in *Axin*$^{\Delta C6/\Delta C6}$ MEFs (derived from homozygous *Axin*$^{\Delta C6/\Delta C6}$ embryos "rescued" by removal of one *Ctnnb1* allele; see below) (Figure 1F, lane 3). This suggests that in *Axin*$^{\Delta C6/+}$ heterozygotes, Axin-ΔC6 may be partially stabilized by dimerization with wild-type Axin.

The deletion of the RGS domain compensates in size for the addition of the Myc tags, so that the Myc-tagged Axin-ΔRGS protein comigrates with untagged wild-type Axin on SDS-polyacrylamide gels (Figure 1H, lane 6). Therefore, we examined the level of Myc-Axin-ΔRGS protein in compound heterozygotes with the *Axin*^{Ax} allele (Figure 1H, lanes 4 and 5). This showed that Myc-Axin-ΔRGS is present in embryos at a level only slightly lower than wild-type Myc-Axin (average 80%). Thus, unlike the C6 deletion, removal of the RGS domain does not significantly affect the steady-state level of the mutant Axin protein.

Embryonic recessive lethality of the *Axin*$^{\Delta RGS}$ allele: Although the dominant-negative activity of Axin-ΔRGS in frog embryo and cell culture assays suggested that it might cause dominant defects in mutant mice (Zeng *et al.* 1997; Fagotto *et al.* 1999), *Axin*$^{\Delta RGS/+}$ heterozygous mice did not display visible abnormalities. *Axin*$^{\Delta RGS/+}$ mice were normally fertile, and backcrosses to wild-type mice generated heterozygous offspring at the expected frequency. However, in homozygotes, the *Axin*$^{\Delta RGS}$ allele caused recessive embryonic defects very similar to those caused by a null allele, *Axin*^{Tg1} (Perry *et al.* 1995; Zeng *et al.* 1997). Embryos from intercrosses among *Axin*$^{\Delta RGS/+}$ mice were examined at E9.5, and *Axin*$^{\Delta RGS/\ \Delta RGS}$ homozygotes were found at the expected frequency (5/22),

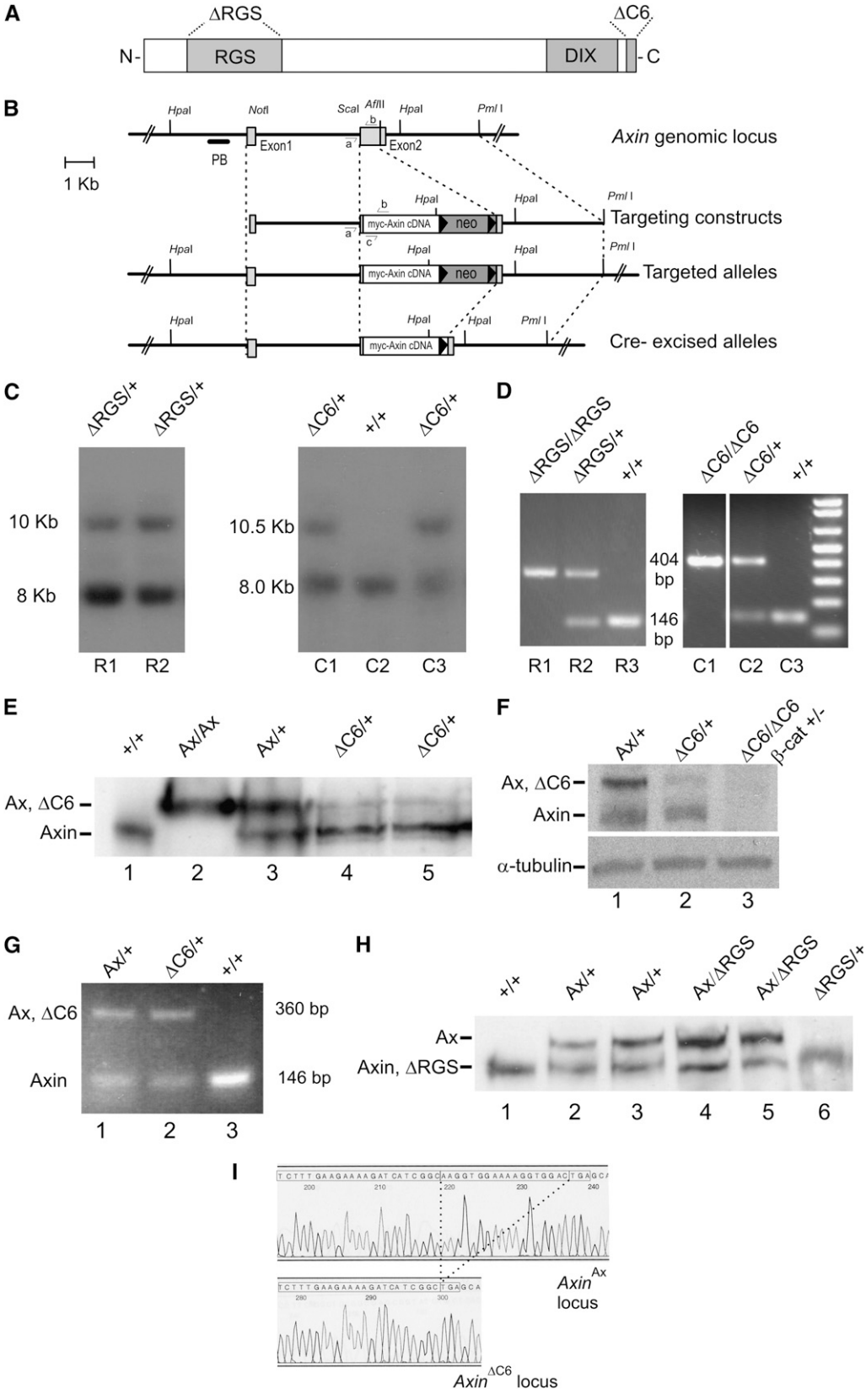

FIGURE 1.—Generation of Axin ΔRGS and AxinΔC6 knockin mice and analysis of mutant Axin expression. (A) Diagram of Axin protein, showing the conserved RGS and DIX domains and the six C-terminal amino acids (KVEKVD). The RGS and C6 domains were deleted in the $Axin^{\Delta RGS}$ and $Axin^{\Delta C6}$ alleles. (B) Diagram of the Axin genomic locus, targeting constructs, and targeted alleles before and after Cre-mediated excision of PGK-neo. The Myc-tagged Axin cDNA contained either the ΔRGS or ΔC6 deletion. Exons 1 and 2 are depicted as lightly shaded boxes, and introns as solid lines. The positions of the restriction enzyme sites and the probe PB used for Southerns are indicated. Small harpoons show the PCR primers AXL1 (A), MTAXR1 (B), and AXL2 (C). (C) Southern blot analysis of G418-resistant colonies after electroporation of ES cells with targeting constructs. Hybridization with probe PB, following digestion of DNA with *Hpa*I, detected bands of 10 kb for the $Axin^{\Delta RGS}$ allele, 10.5 kb for the $Axin^{\Delta C6}$ allele, and 8 kb for the wild-type (+/+) allele. (D) Identification of homozygous and heterozygous $Axin^{\Delta RGS}$ or $Axin^{\Delta C6}$ mice, and wild-type mice by PCR using primers AXL1 and MTAXR1. (E) Protein expression in a wild type (lane 1), an $Axin^{Ax/Ax}$ (lane 2), an $Axin^{Ax/+}$ (lane 3), and two different $Axin^{\Delta C6/+}$ (lanes 4 and 5) mouse embryos by Western blotting with a polyclonal anti-Axin antibody. The lower bands in lanes 1, 3, 4, and 5 are endogenous Axin (110 kDa), while the upper bands (~130 kDa) are the Myc-tagged wild-type Axin or Myc-tagged Axin-ΔC6 (which differ by only six amino acids and comigrate). The $Axin^{Ax/+}$ heterozygote expressed similar amounts of Myc-tagged Axin from the $Axin^{Ax}$ allele and endogenous Axin (lane 3). However, Myc-tagged Axin-ΔC6 was expressed approximately three- to fourfold lower than endogenous Axin from the normal allele (lanes 4 and 5). (F) Protein expression in MEFs derived from embryos of the indicated genotypes. Myc-tagged Axin-ΔC6 was not detected in MEFs from a homozygous $Axin^{\Delta C6/\Delta C6}$ embryo rescued by absence of one β-catenin allele (lane 3). α-tubulin was used as a loading control. (G) Comparison of mRNA expression levels by RT–PCR, in mouse embryonic fibroblasts derived from wild type, $Axin^{Ax/+}$ and $Axin^{\Delta C6/+}$ heterozygotes, using primers AXL2 and

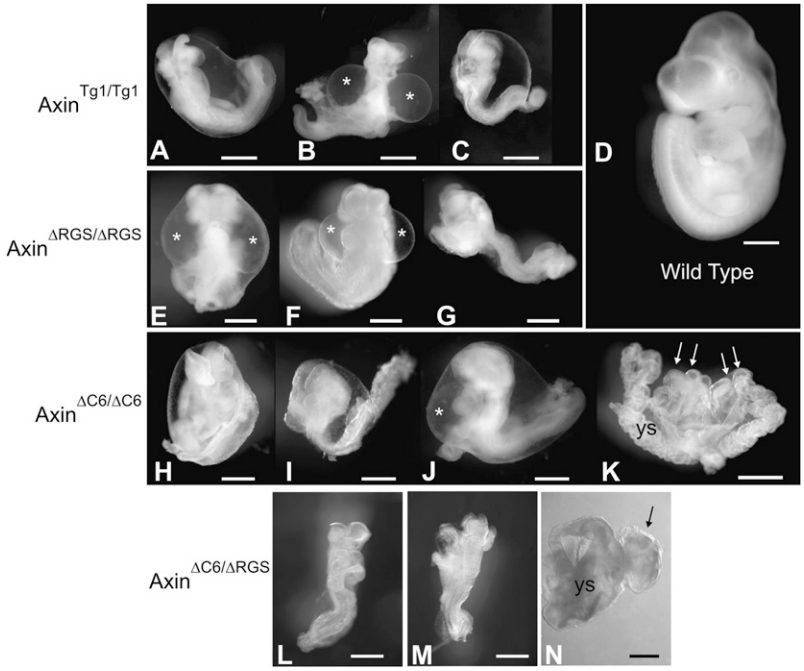

FIGURE 2.—*Axin*$^{\Delta RGS}$ or *Axin*$^{\Delta C6}$ homozygotes and *Axin*$^{\Delta C6/\Delta RGS}$ compound heterozygotes display an embryonic lethal phenotype indistinguishable from that of the null allele *Axin*^{Tg1}. (A–C) E9.5 *Axin*^{Tg1} homozygous embryos. (D) Wild-type E9.5 embryo at same magnification. (E–G) E9.5 *Axin*$^{\Delta RGS}$ homozygous embryos. (H–K) E9.5 *Axin*$^{\Delta C6}$ homozygous embryos. Most embryos homozygous for any of the three mutations displayed reduced size and developmental delay, open head folds and truncated heads. Other common features illustrated here are cardia bifida and enlarged pericardia (asterisks). The embryo in K has duplicated axes, as sometimes observed in the original *Axin*^{Tg1} mutant (PERRY *et al.* 1995; ZENG *et al.* 1997). The arrows point to two sets of head folds within the same yolk sac (ys). (L–N) E9.5 *Axin*$^{\Delta C6/\Delta RGS}$ compound heterozygous embryos. The embryos in L and M are delayed and show open head folds; the embryo in N (arrow) is located outside the yolk sac, a property of some *Axin*^{Tg1} homozygous embryos (PERRY *et al.* 1995). ys, yolk sac. Bars, 0.5 mm.

but all were severely abnormal (Figure 2, E–G) and indistinguishable from homozygotes for the null *Axin*^{Tg1} allele (Figure 2, A–C). They were much smaller than wild-type or heterozygous littermates (Figure 2D) and displayed characteristic abnormalities also seen in null *Axin*$^{Tg1/Tg1}$ embryos (PERRY *et al.* 1995), including a severely underdeveloped trunk, kinky neural tube, failure to turn, open and shortened head folds, enlarged pericardium, and cardia bifida.

Loss of the Axin C6 motif results in recessive embryonic lethality: *Axin*$^{\Delta C6/+}$ heterozygotes appeared normal, fertile, and transmitted the *Axin*$^{\Delta C6}$ allele at a frequency of ~50%. However, *Axin*$^{\Delta C6/\Delta C6}$ homozygous mice could not be generated. Of 22 F_2 pups obtained at weaning from *Axin*$^{\Delta C6/+}$ intercrosses, 12 were *Axin*$^{\Delta C6/+}$ while the remaining 10 were wild type. Since we had not noted any postnatal death, we concluded that *Axin*$^{\Delta C6}$ was likely to be prenatal recessive lethal allele.

Axin$^{\Delta C6/\Delta C6}$ embryos were examined at E9.5 to -10.5, stages at which the *Axin*$^{Tg1/Tg1}$ null homozygotes were severely abnormal but not yet resorbed (PERRY *et al.* 1995; ZENG *et al.* 1997). There were 32/137 mutant homozygotes, consistent with the expected 25% frequency, and all were severely abnormal (Figure 2, H–K). In addition to being much smaller than wild-type littermates, they were indistinguishable from *Axin*$^{Tg1/Tg1}$ (or *Axin*$^{\Delta RGS/\Delta RGS}$) embryos, displaying the same characteristic features, including reduced size (32/32), open and shortened head folds (14/32), cardia bifida (14/32), enlarged pericardium (13/32), kinky neural tube (10/32), and duplicated body axes (1/32) (PERRY *et al.* 1995; ZENG *et al.* 1997). Therefore, we conclude that *Axin*$^{\Delta C6}$ also acts essentially as a null allele.

The Axin-ΔC6 protein is fully active in the canonical Wnt pathway: The recessive lethality of the *Axin*$^{\Delta C6}$ allele could be due to inherent defects in mutant Axin-ΔC6 protein (in its ability either to regulate the canonical Wnt pathway or to carry out some other, unknown, function of Axin), or else they might be due simply to the low level of the mutant Axin protein. To try to distinguish between these explanations, we performed a number of experiments to analyze the properties of the Axin-ΔC6 protein. First, to rule out the trivial explanation that we had made the wrong mutation, we verified the presence of the expected targeted mutation at the *Axin* locus by sequencing a PCR product generated from genomic DNA prepared from *Axin*$^{\Delta C6/\Delta C6}$ embryos (Figure 1I). This confirmed that the mutation was as expected.

It was previously reported that deletion of the C6 motif does not impair the ability of Axin to attenuate LEF1 luciferase reporter activity, or to reduce the cellular β-catenin level when cotransfected with β-catenin (RUI *et al.* 2002). We confirmed that Axin-ΔC6 is indistin-

MTAXR1. The *Axin*$^{\Delta C6}$ allele (which produces a larger, 360-bp band, due to the presence of the Myc-tag) is expressed at the same level as the wild-type allele (146-bp band). (H) Protein expression in wild type (lane 1), *Axin*$^{Ax/+}$ (lanes 2 and 3), *Axin*$^{Ax/\Delta RGS}$ (lanes 4 and 5), and *Axin*$^{\Delta RGS/+}$ mouse embryos (lane 6) by Western blotting with a polyclonal anti-Axin antibody. Myc-tagged Axin-ΔRGS comigrates with endogenous Axin (lane 6) because of the opposite effects on size of the Myc tags and the RGS deletion. Therefore, the level of Axin-ΔRGS protein was examined using *Axin*$^{Ax/\Delta RGS}$ compound heterozygotes, in which wild-type Myc-Axin is the upper band and Myc-Axin-ΔRGS is the lower band. (I) Confirmation of the 18-bp deletion in the Axin$^{\Delta C6}$ allele by DNA sequencing.

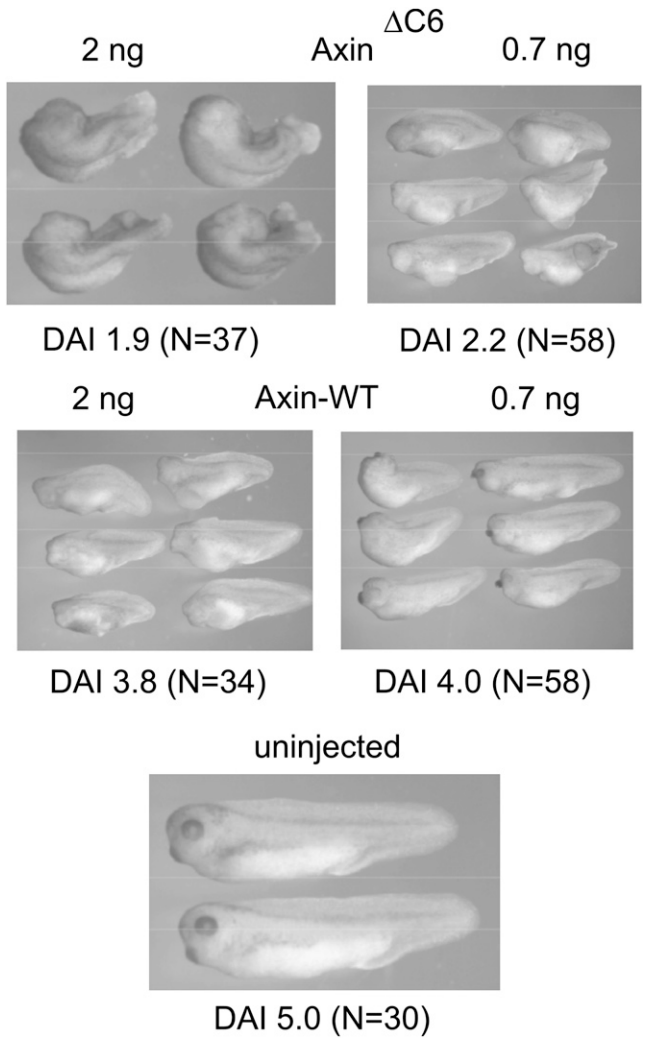

Figure 3.—Ability of Axin-ΔC6 to inhibit axis formation in frog embryos. Injection of Axin-ΔC6 RNA into dorsal blastomeres of four-cell stage Xenopus embryos resulted in ventralization. Axin-ΔC6 and full-length Axin were tested at two different concentrations, and Axin-ΔC6 displayed a somewhat increased activity in this assay. DAI, dorsoanterior index: 5 is normal and 1 is the most strongly ventralized.

guishable from wild-type Axin in its ability to negatively regulate a LEF1 luciferase reporter when cotransfected into 293 cells along with β-catenin (data not shown). To confirm in a different assay that the Axin-ΔC6 protein is fully functional in the canonical Wnt pathway, we examined its ability to ventralize Xenopus embryos when its mRNA was injected into the dorsal side of four cell-stage Xenopus embryos, an established assay for proteins that inhibit the Wnt pathway. The results indicated that the Axin-ΔC6 protein is capable of promoting β-catenin degradation. In fact, surprisingly, Axin-ΔC6 had stronger ventralizing effects than full-length Axin, at two different dosages (Figure 3). Thus, we conclude that the defects of $Axin^{\Delta C6/\Delta C6}$ mutant embryos are not due to any inherent inability of this truncated protein to inhibit the canonical Wnt pathway when overexpressed.

The recessive embryonic lethality of the $Axin^{\Delta C6}$ allele is due to a failure to regulate the level of β-catenin *in vivo*: As a genetic test of its activity in the canonical Wnt/β-catenin pathway, we attempted to rescue the embryonic lethality of $Axin^{\Delta C6/\Delta C6}$ mutants by making them heterozygous for a β-catenin null allele ($Ctnnb1^{+/-}$), and thus reducing the level of β-catenin. If the lethality was due to failure of $Axin^{\Delta C6}$ to regulate the β-catenin level, resulting in its excessive accumulation, then reducing the *Ctnnb1* gene dosage might compensate and thus partially correct the phenotypic defects. On the other hand, if the lethality were due to the effects of this Axin mutation on a different signaling pathway, then reducing the *Ctnnb1* gene dosage should have no effect.

Surprisingly, we found that removal of one allele of *Ctnnb1* was able to completely rescue the embryonic lethality caused by the $Axin^{\Delta C6}$ allele. While $Axin^{\Delta C6/\Delta C6}$ embryos were all severely abnormal by E9.5 and resorbed by E11.5, $Axin^{\Delta C6/\Delta C6}$; $Ctnnb1^{+/-}$ compound mutants were able to develop to the end of gestation (E18.5, when they were sacrificed). We obtained two $Axin^{\Delta C6/\Delta C6}$; $Ctnnb1^{+/-}$ compound mutants at this stage, both of which had apparently normal bodies, while only the face and head were abnormal (Figure 4, A and B, left). One had a mild cleft lip and a protruding tongue (Figure 4A, left), and the other had more severe facial clefting, with the brain protruding from the oral cavity above the tongue (Figures 4B, left). Sectioning of the mutant embryo in Figure 4B (left) revealed multiple abnormalities, including cleft palate (arrows), absence of nasal structures (asterisk), and multiple brain malformations (Figure 4C, left).

To examine the developmental timing of the craniofacial abnormalities in these "rescued" $Axin^{\Delta C6/\Delta C6}$; $Ctnnb1^{+/-}$ mutants, additional embryos were examined at earlier prenatal stages. The facial defects could be traced back to E11.5, when impaired fusion of the medial nasal prominences was already visible (not shown). Figure 4D (left) shows an example of a rescued mutant at E14.5, in which the facial prominences failed to fuse. These defects were never seen in any other genotypic combination, nor were $Axin^{\Delta C6/\Delta C6}$ embryos not carrying the *Ctnnb1* mutant allele found at E11.5 or later.

In conclusion, the ability to rescue the pre-E10.5 embryonic lethality of the $Axin^{\Delta C6/\Delta C6}$ mutant embryos by reducing the *Ctnnb1* gene dosage strongly suggests that the early lethality of the $Axin^{\Delta C6/\Delta C6}$ mutants is due to a deficiency in regulating the Wnt/β-catenin pathway. Thus, while the mutant protein is capable of regulating this pathway when overexpressed, it fails to do so in the homozygous mutant embryos, presumably because it is present at too low a level.

To ask if reduced JNK activity might contribute to the craniofacial defects of $Axin^{\Delta C6/\Delta C6}$; $Ctnnb1^{+/-}$ compound mutants, we performed JNK assays on UV-irradiated MEFs isolated from $Axin^{\Delta C6/\Delta C6}$; $Ctnnb1^{+/-}$ and control

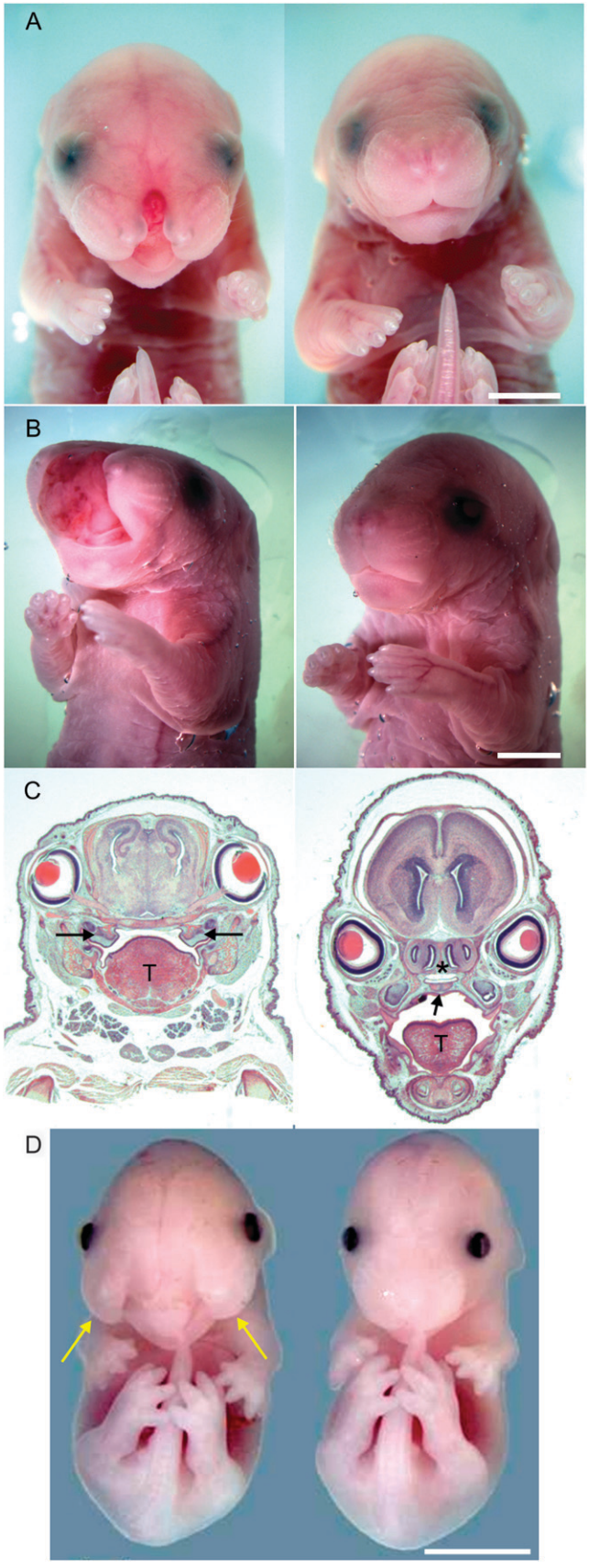

E13.5 embryos, but saw no differences in JNK activity (data not shown). While this did not rule out a role for JNK activation by Axin, it failed to provide support for this hypothesis.

The $Axin^{\Delta C6}$ and $Axin^{\Delta RGS}$ alleles fail to complement each other: Since Axin is believed to function as a dimer, it was possible that intragenic complementation between two different embryonic lethal alleles might partially or fully rescue embryonic development. If the reduced amount of Axin-ΔC6 protein were sufficient to support development, but the protein were functionally defective (*i.e.*, if the last six amino acids were important for functions other than stability), it might be able to complement a different deletion allele, via dimerization between the two mutant proteins. To test this possibility, $Axin^{\Delta C6/+}$ and $Axin^{\Delta RGS/+}$ mice were crossed. No compound heterozygotes were found among 30 live-born progeny, nor among 30 conceptuses recovered at E12.5. At E12.5, none of the 20 live embryos were compound heterozygotes, and there were 10 empty decidua (whose contents could not be genotyped), suggesting that the compound mutant embryos had already been resorbed. At E9.5, 7/29 embryos were $Axin^{\Delta C6/\Delta RGS}$ compound heterozygotes, and all were developmentally delayed and phenotypically similar to homozygotes for the $Axin^{Tg1}$, $Axin^{\Delta C6}$, or $Axin^{\Delta RGS}$ alleles (Figure 2, L, M, and N). Thus, $Axin^{\Delta C6/\Delta RGS}$ compound heterozygotes die at the same stage as homozygotes for either mutation. While the failure to complement does not exclude a functional defect in the Axin-ΔC6 protein, it is consistent with the interpretation that embryonic lethality is due to the low level of Axin-ΔC6 protein.

DISCUSSION

In this study, we used targeted gene replacement in mice to investigate the *in vivo* significance of two conserved domains of Axin, the APC-binding (RGS) domain and the terminal C6 motif (KVEKVD). While this strategy is more laborious than many other experimental approaches, it has the advantage that it preserves the normal pattern and level of transcription of the endogenous locus, while also knocking out the

FIGURE 4.—Reduction of the β-catenin gene dosage rescues the early lethality of $Axin^{\Delta C6}$ homozygotes, but the mutant animals display craniofacial defects. The individuals on the left are homozygous for the $Axin^{\Delta C6}$ allele and heterozygous for *Ctnnb1* (β-catenin) null allele, while those on the right are wild-type littermates. (A and B) At E18.5, the "rescued" $Axin^{\Delta C6}$ mutants display severe clefting of the face, sometimes with a protruding brain (B), but the rest of the body appears normal. (C) A histological section of the rescued mutant mouse in B reveals cleft palate (arrows), absence of nasal structures seen in the wild type (asterisk), and severe brain abnormalities. (D) Failure of the facial prominences to fuse (arrows) in a rescued mutant at E14.5.

endogenous gene. Therefore, mutant forms of the protein are assayed for their functions *in vivo*, and in the absence of the endogenous gene product. We found that the RGS domain and the C6 motif are both required for the normal activity of Axin, as homozygotes for either deletion allele displayed embryonic lethality and abnormalities indistinguishable from those caused by a null allele. However, the mechanisms by which they disrupt the function of Axin appear to be different.

The RGS domain is required for binding to APC *in vitro*, but there were conflicting data regarding its importance for the function of Axin in the canonical Wnt pathway (Zeng *et al.* 1997; Hart *et al.* 1998; Ikeda *et al.* 1998). Our finding that $Axin^{\Delta RGS/\Delta RGS}$ mutants resemble null $Axin^{Tg1/Tg1}$ embryos at E9.5 confirms that the RGS domain is required for the functions of Axin *in vivo*, presumably because it is needed to interact with APC (although other potential functions of the RGS domain cannot be excluded). Although Axin lacking its RGS domain acts as a dominant-negative in frog embryo and cell transfection assays (Zeng *et al.* 1997; Fagotto *et al.* 1999), we did not observe any abnormalities in heterozygous $Axin^{\Delta RGS/+}$ animals. This may be because the amount of the mutant protein in heterozygous mice is lower than it is in typical overexpression experiments, and it is therefore insufficient to inhibit the endogenous wild-type Axin.

Our interest in the C6 motif of Axin stemmed from a report that overexpression of Axin in HEK293 cells could activate the JNK MAP kinase through the upstream kinases MEKK1 and MEKK4 (Zhang *et al.* 1999, 2000, 2001; Rui *et al.* 2002). Deletion analysis revealed that the two domains required for JNK activation are different from those needed for Wnt regulation. They included a region needed for Axin homodimerization (between residues 507 and 832) as well as the C6 motif. Thus, deletion of only C6 severely reduced the ability of Axin to activate JNK, but not to regulate β-catenin levels, in transfected cells. It was also shown that C6 is a major site for SUMOylation of Axin (Rui *et al.* 2002), a modification whose significance remains unclear, although we have obtained evidence that SUMOylation of the C6 motif may protect Axin from ubiquitination (Kim *et al.* 2008). We found that the $Axin^{\Delta C6}$ allele was also recessive lethal, and that $Axin^{\Delta C6/\Delta C6}$ embryos died at the same stage as null $Axin^{Tg1/Tg1}$ mutants, with the same spectrum of defects. However, this embryonic lethality appears most likely to be due to a low level of expression of the Axin-ΔC6 protein, rather than to any inherent functional defect in the mutant protein, for the following reasons.

First, in heterozygous embryos, where the level of Axin-ΔC6 protein should have been equivalent to wild-type Axin, it was present at three- to fourfold lower levels, while in homozygous mutant embryos it was undetectable (probably <10% of wild-type levels). Subsequent biochemical experiments have shown that the removal of the C6 motif results in increased ubiquitination and decreased stability of Axin-ΔC6, apparently due to the loss of the SUMOylation sites within the C6 motif (Kim *et al.* 2008).

Second, Axin-ΔC6 showed a normal capacity to attenuate a Lef1-luciferase reporter in transfected cells, and a somewhat enhanced ability to ventralize frog embryos when injected dorsally at the four-cell stage. Both of these assays may be relatively insensitive to the stability of the protein; however, they have been used extensively to define functional domains of Axin, and other proteins involved in canonical Wnt signaling, so any inherent defect in the ability of Axin-ΔC6 to regulate this pathway probably would have been apparent in these experiments.

Third, the embryonic lethality of $Axin^{\Delta C6/\Delta C6}$ mutants could be rescued by eliminating one allele of the β-catenin gene *Ctnnb1*, and these rescued mutants developed to term with craniofacial defects, but no other gross abnormalities. This provided genetic proof that the early lethality and multiple abnormalities at E9.5–E10.5 are due to failure of the $Axin^{\Delta C6}$ allele to negatively regulate the level of β-catenin. Further evidence that the embryonic lethality of both $Axin^{Tg1/Tg1}$ and $Axin^{\Delta C6/\Delta C6}$ mutants can be explained by failure to regulate the Wnt/β-catenin pathway comes from the observation that overexpression of cWnt8c in the mouse embryo resulted in a very similar embryonic lethal phenotype (Pöpperl *et al.* 1997). Since the Axin-ΔC6 protein is *capable* of regulating β-catenin levels when overexpressed but fails to do so in homozygous mutant embryos, the simplest explanation is its low level of expression.

Although the embryonic lethality of $Axin^{\Delta C6/\Delta C6}$ mutants was rescued by reducing the level of β-catenin, the rescued animals displayed severe craniofacial abnormalities. These residual defects in craniofacial development could be due either to incomplete rescue of the excessive β-catenin signaling or to a failure of $Axin^{\Delta C6}$ to perform a different function.

According to the first model, strongly elevated levels of β-catenin cause the embryonic lethal phenotype, while mildly elevated levels cause only craniofacial defects. Evidence consistent with this model comes from analysis of compound mutant mice between *Axin* and *Axin2*. While homozygous *Axin2*−/− mice develop normally except for skull malformations (caused by premature fusion of cranial sutures) (Yu *et al.* 2005), *Axin2*−/− embryos that were also missing one *Axin* allele were born with severe craniofacial abnormalities reminiscent of those seen in the rescued $Axin^{\Delta C6/\Delta C6}$; $Ctnnb1^{+/-}$ mutants. Furthermore, the defects in *Axin2*−/−; *Axin*+/− mice could be fully rescued by deletion of one allele of *Ctnnb1* (B. Jerchow and W. Birchmeier, personal communication). Therefore, the evidence suggests that there may be a continuum of defects, ranging from embryonic lethality, to survival

with craniofacial defects, to normal development, depending on the level of depletion of Axin and/or Axin2 and the consequent deregulation of β-catenin. This might be directly tested in the future by manipulating the levels of β-catenin in developing embryos. The ability of the *Axin*$^{\Delta C6/\Delta C6}$ mutants to be rescued by reduction in β-catenin gene dosage was sensitive to genetic background (data not shown), suggesting that other genes that vary between inbred strains of mice may also affect the level of β-catenin signaling.

According to the second model, Axin might be important not only to negatively regulate β-catenin, but also, later in development, to perform another function. One such function might be related to its capacity to stimulate the JNK pathway via the C6 motif (Rui *et al.* 2002). If this were true, one might expect knockout of JNK genes to result in defects similar to those caused by A*xin*$^{\Delta C6}$. Of the three JNK genes, *Mapk8* (JNK1) and *Mapk9* (JNK2) are ubiquitously expressed while *Mapk10* (JNK3) is expressed in the CNS (Kuan *et al.* 1999; Weston and Davis 2002). Single knockouts of *Mapk8*, *Mapk9*, or *Mapk10* cause only minor defects, none affecting craniofacial development (Yang *et al.* 1997; Kuan *et al.* 1999; Sabapathy *et al.* 1999; Weston and Davis 2002). Simultaneous loss of *Mapk8* and J *Mapk9* NK2 results in exencephaly and neural tube closure defects due to reduced apoptosis in the hindbrain (Kuan *et al.* 1999), while *Mapk8/Mapk10* and *Mapk9/Map10* double mutants are viable (Yang *et al.* 1997; Kuan *et al.* 1999). However, the triple mutant has not been reported, so a role in craniofacial development has not been fully excluded.

It has recently been shown that JNK signaling in early Xenopus embryos can antagonize the canonical Wnt pathway, apparently by regulating the nucleocytoplasmic transport of β-catenin (Liao *et al.* 2006). Therefore, any potential effects of Axin on JNK signaling may not be completely separable from its effects on β-catenin. Furthermore, Axin can interact with proteins involved in several signaling pathways (*e.g.*, TGF-β), so we cannot exclude the additional possibility that the incomplete rescue of *Axin*$^{\Delta C6/\Delta C6}$ by the β-catenin heterozygous deletion reflects a role for Axin in some other pathway. Regardless of the mechanism, the Axin-$^{\Delta C6}$ mutation establishes that the C6 motif has an essential function *in vivo*. This may be related to its ability to protect Axin from ubiquitination and instability (Kim *et al.* 2008).

We thank Chyuan-Sheng Lin for the CSL3 embryonic stem cells and David Virshup for the anti-Axin antiserum. This work was supported by Public Health Service grants HD-44265 to F.C. and HD-31247 to S.S., from the National Institute of Child Health and Human Development.

LITERATURE CITED

Aulehla, A., C. Wehrle, B. Brand-Saberi, R. Kemler, A. Gossler *et al.*, 2003 Wnt3a plays a major role in the segmentation clock controlling somitogenesis. Dev. Cell **4:** 395–406.

Behrens, J., B. A. Jerchow, M. Wurtele, J. Grimm, C. Asbrand *et al.*, 1998 Functional interaction of an axin homolog, conductin, with beta- catenin, APC, and GSK3beta. Science **280:** 596–599.

Brault, V., R. Moore, S. Kutsch, M. Ishibashi, D. H. Rowitch *et al.*, 2001 Inactivation of the beta-catenin gene by Wnt1-Cre-mediated deletion results in dramatic brain malformation and failure of craniofacial development. Development **128:** 1253–1264.

Chia, I. V., and F. Costantini, 2005 Mouse axin and axin2/conductin proteins are functionally equivalent in vivo. Mol. Cell. Biol. **25:** 4371–4376.

Fagotto, F., E. Jho, L. Zeng, T. Kurth, T. Joos *et al.*, 1999 Domains of axin involved in protein-protein interactions, wnt pathway inhibition, and intracellular localization. J. Cell Biol. **145:** 741–756.

Hart, M. J., R. de los Santos, I. N. Albert, B. Rubinfeld and P. Polakis, 1998 Downregulation of beta-catenin by human Axin and its association with the APC tumor suppressor, beta-catenin and GSK3 beta. Curr. Biol. **8:** 573–581.

Hsu, W., L. Zeng and F. Costantini, 1999 Identification of a domain of axin that binds to the Serine/Threonine protein phosphatase 2A and a self-binding domain. J. Biol. Chem. **274:** 3439–3445.

Ikeda, S., S. Kishida, H. Yamamoto, H. Murai, S. Koyama *et al.*, 1998 Axin, a negative regulator of the Wnt signaling pathway, forms a complex with GSK-3beta and beta-catenin and promotes GSK-3beta- dependent phosphorylation of beta-catenin. EMBO J. **17:** 1371–1384.

Itoh, K., V. E. Krupnik and S. Y. Sokol, 1998 Axis determination in Xenopus involves biochemical interactions of axin, glycogen synthase kinase 3 and beta-catenin. Curr. Biol. **8:** 591–594.

Jho, E., S. Lomvardas and F. Costantini, 1999 A GSK3beta phosphorylation site in axin modulates interaction with beta-catenin and Tcf-mediated gene expression. Biochem. Biophys. Res. Commun. **266:** 28–35.

Jho, E. H., T. Zhang, C. Domon, C. K. Joo, J. N. Freund *et al.*, 2002 Wnt/beta-catenin/Tcf signaling induces the transcription of Axin2, a negative regulator of the signaling pathway. Mol. Cell. Biol. **22:** 1172–1183.

Julius, M. A., B. Schelbert, W. Hsu, E. Fitzpatrick, E. Jho *et al.*, 2000 Domains of axin and disheveled required for interaction and function in wnt signaling. Biochem. Biophys. Res. Commun. **276:** 1162–1169.

Kao, K. R., and R. P. Elinson, 1988 The entire mesodermal mantle behaves as Spemann's organizer in dorsoanterior enhanced Xenopus laevis embryos. Dev. Biol. **127:** 64–77.

Kim, M. J., I. V. Chia and F. Costantini, 2008 SUMOylation target sites at the C terminus protect Axin from ubiquitination and confer protein stability. FASEB J. **22:** 3785–3794.

Kishida, S., H. Yamamoto, S. Hino, S. Ikeda, M. Kishida *et al.*, 1999 DIX domains of dvl and axin are necessary for protein interactions and their ability to regulate beta-catenin stability. Mol. Cell. Biol. **19:** 4414–4422.

Korinek, V., N. Barker, P. J. Morin, D. van Wichen, R. de Weger *et al.*, 1997 Constitutive transcriptional activation by a beta-catenin-Tcf complex in APC−/− colon carcinoma. Science **275:** 1784–1787.

Kuan, C. Y., D. D. Yang, D. R. Samanta Roy, R. J. Davis, P. Rakic *et al.*, 1999 The Jnk1 and Jnk2 protein kinases are required for regional specific apoptosis during early brain development. Neuron **22:** 667–676.

Lewandoski, M., 2001 Conditional control of gene expression in the mouse. Nat. Rev. Genet. **2:** 743–755.

Lewandoski, M., and G. R. Martin, 1997 Cre-mediated chromosome loss in mice. Nat. Genet. **17:** 223–225.

Li, L., H. Yuan, C. D. Weaver, J. Mao, G. H. Farr, 3rd *et al.*, 1999 Axin and Frat1 interact with dvl and GSK, bridging Dvl to GSK in Wnt-mediated regulation of LEF-1. EMBO J. **18:** 4233–4240.

Liao, G., Q. Tao, M. Kofron, J. S. Chen, A. Schloemer *et al.*, 2006 NH2-terminal kinase (JNK) prevents nuclear beta-catenin accumulation and regulates axis formation in Xenopus embryos. Proc. Natl. Acad. Sci. USA **103:** 16313–16318.

Luo, W., and S. C. Lin, 2004 Axin: a master scaffold for multiple signaling pathways. Neurosignals **13:** 99–113.

Lustig, B., B. Jerchow, M. Sachs, S. Weiler, T. Pietsch *et al.*, 2002 Negative feedback loop of Wnt signaling through upregulation of conductin/axin2 in colorectal and liver tumors. Mol. Cell. Biol. **22:** 1184–1193.

Mao, J., J. Wang, B. Liu, W. Pan, G. H. Farr, III *et al.*, 2001 Low-density lipoprotein receptor-related protein-5 binds to Axin and regulates the canonical Wnt signaling pathway. Mol. Cell **7:** 801–809.

Munemitsu, S., I. Albert, B. Souza, B. Rubinfeld and P. Polakis, 1995 Regulation of intracellular beta-catenin levels by the adenomatous polyposis coli (APC) tumor-suppressor protein. Proc. Natl. Acad. Sci. USA **92:** 3046–3050.

Perry, W. L. I., T. J. Vasicek, J. J. Lee, J. M. Rossi, L. Zeng *et al.*, 1995 Phenotypic and molecular analysis of a transgenic insertional allele of the mouse *Fused* locus. Genetics **141:** 321–332.

Pöpperi, H., C. Schmidt, V. Wilson, C. R. Hume, J. Dodd *et al.*, 1997 Misexpression of Cwnt8C in the mouse induces an ectopic embryonic axis and causes a truncation of the anterior neurectoderm. Development **124:** 2997–3005.

Rui, H. L., E. Fan, H. M. Zhou, Z. Xu, Y. Zhang *et al.*, 2002 SUMO-1 modification of the C-terminal KVEKVD of Axin is required for JNK activation but has no effect on Wnt signaling. J. Biol. Chem. **277:** 42981–42986.

Sabapathy, K., W. Jochum, K. Hochedlinger, L. Chang, M. Karin *et al.*, 1999 Defective neural tube morphogenesis and altered apoptosis in the absence of both JNK1 and JNK2. Mech. Dev. **89:** 115–124.

Salahshor, S., and J. R. Woodgett, 2005 The links between axin and carcinogenesis. J. Clin. Pathol. **58:** 225–236.

Weston, C. R., and R. J. Davis, 2002 The JNK signal transduction pathway. Curr. Opin. Genet. Dev. **12:** 14–21.

Xing, Y., W. K. Clements, D. Kimelman and W. Xu, 2003 Crystal structure of a beta-catenin/axin complex suggests a mechanism for the beta-catenin destruction complex. Genes Dev. **17:** 2753–2764.

Yamamoto, H., S. Kishida, M. Kishida, S. Ikeda, S. Takada *et al.*, 1999 Phosphorylation of Axin, a Wnt signal negative regulator, by glycogen synthase kinase-3beta regulates its stability. J. Biol. Chem. **274:** 10681–10684.

Yang, D. D., C. Y. Kuan, A. J. Whitmarsh, M. Rincon, T. S. Zheng *et al.*, 1997 Absence of excitotoxicity-induced apoptosis in the hippocampus of mice lacking the Jnk3 gene. Nature **389:** 865–870.

Yu, H. M., B. Jerchow, T. J. Sheu, B. Liu, F. Costantini *et al.*, 2005 The role of Axin2 in calvarial morphogenesis and craniosynostosis. Development **132:** 1995–2005.

Zeng, L., F. Fagotto, T. Zhang, W. Hsu, T. J. Vasicek *et al.*, 1997 The mouse *Fused* locus encodes Axin, an inhibitor of the Wnt signaling pathway that regulates embryonic axis formation. Cell **90:** 181–192.

Zhang, Y., S. Y. Neo, J. Han and S. C. Lin, 2000 Dimerization choices control the ability of axin and dishevelled to activate c-Jun N-terminal kinase/stress-activated protein kinase. J. Biol. Chem. **275:** 25008–25014.

Zhang, Y., S. Y. Neo, X. Wang, J. Han and S. C. Lin, 1999 Axin forms a complex with MEKK1 and activates c-Jun NH(2)-terminal kinase/stress-activated protein kinase through domains distinct from Wnt signaling. J. Biol. Chem. **274:** 35247–35254.

Zhang, Y., W. J. Qiu, D. X. Liu, S. Y. Neo, X. He *et al.*, 2001 Differential molecular assemblies underlie the dual function of Axin in modulating the WNT and JNK pathways. J. Biol. Chem. **276:** 32152–32159.

Communicating editor: T. R. Magnuson